

Numerical study of spinodal decomposition for Langevin equations

Oriol T. Valls

School of Physics and Astronomy, University of Minnesota, Minneapolis, Minnesota 55455

Gene F. Mazenko

The James Franck Institute, The University of Chicago, Chicago, Illinois 60637

(Received 8 September 1987)

We study the time-dependent Ginzburg-Landau model for spinodal decomposition by numerical solution of the associated Langevin equation. The evolution of the system after deep temperature quenches to many different points in the ordered region of the phase diagram has been followed for time scales that are estimated to be equivalent to at least 10^4 and up to more than 10^5 Monte Carlo steps. Analysis of results obtained for block-correlation functions show that the system exhibits scaling behavior and that the average domain size $L(t)$ grows as $L(t) \sim t^{1/4}$ in the time region covered by the calculations. We have also studied the quasistatic structure factor $C(q, t)$. The results obtained for this quantity are consistent with those obtained for the block correlations, although, in agreement with other authors, we find that results for $C(q, t)$ alone are not conclusive.

I. INTRODUCTION

One path towards an understanding of growth-kinetics phenomena in systems subjected to temperature quenches to unstable regions of their phase diagram has been made through the study of Langevin equations associated with time-dependent Ginzburg-Landau (TDGL) models.¹ Numerical solution of these equations is now possible for time and size scales quite competitive with those that can be achieved with Monte Carlo (MC) simulations. This has the advantage of being able to obtain results for systems with a continuous, rather than a discrete (e.g., Ising or Potts) order parameter. It is expected that reversible model-coupling nonlinearities will play an important role in the growth kinetics of many systems and one can reasonably expect to be able to treat such "hydrodynamic" effects in simple models of nonequilibrium fluids in the near future. In this treatment we restrict ourselves to strictly dissipative models.

We have recently² shown that direct numerical solution of the Langevin equations for a TDGL model containing a single, scalar variable with a nonconserved order parameter (this is model *A* in the taxonomy of Halperin and Hohenberg³) quenched from a high to a low temperature leads to a confirmation of the Lifshitz-Cahn-Allen⁴ law for the growth of the average domain size L with time t [$L(t) \sim t^{1/2}$]. Similar results have been obtained for the same model by the use of Monte Carlo simulations.⁵ Basic questions of numerical methodology and efficiency were also discussed in Ref. 2. In the present work we wish to consider the more important and considerably more complicated case where the order parameter is a conserved quantity⁶ (model *B* in Ref. 3). Although some preliminary results obtained by direct numerical solution of the equations for this system exist in the literature,⁷ these results are not sufficiently accurate to give any information on questions such as the long-time growth law. Results obtained for this model

through direct MC simulation⁸ are also ambiguous in this respect.

In this paper we report results obtained by numerical integration of the model *B* Langevin equation subjected to a sudden, deep temperature quench. The results are of sufficient quality to determine the growth law for the regime investigated. The results for an "average" domain size $L(t)$, which extend to times which are quite considerable when measured in a MC time scale, are determined in two different ways. The first consists of studying a set of block-correlation functions and analyzing their behavior as a function of time and block size. In addition to its theoretical advantages, we shall see that this method is very efficient from a computational point of view. We have also used the more conventional method of studying the moments or maxima of the quasistatic-structure factor, $C(q, t)$. Scaling behavior is established by using the first method, which leads to the result $L(t) \sim t^{1/4}$. This power law is confirmed by the second method.

The model considered here can also be treated analytically at very low temperatures. The methods developed in this approach are very involved and will be reported in a separate paper,⁹ but they lead also to a $\frac{1}{4}$ power at long times.

The result of $\frac{1}{4}$ for the exponent does not agree with the widely expected value of $\frac{1}{3}$ which one obtains through the use of the Lifshitz-Slyozov¹⁰ theory. Of course, in any numerical calculation such as this one, it is not possible to completely rule out the possibility that the observed behavior is only a persistent transient and that there is a later crossover to the $\frac{1}{3}$ value (which is not very different from $\frac{1}{4}$). Such a crossover has been reported¹¹ for a different model in the soft-wall case. Within the ranges studied here, we see no signs of such a crossover in either the hard- or soft-wall case. In the analytic treatment of Ref. 9, an exponent of $\frac{1}{3}$ could result, e.g., from corrections to the $\frac{1}{4}$ result of higher order in the temperature. There is some evidence for a $\frac{1}{4}$ exponent from simu-

lations of a Lennard-Jones system (see Ref. 12).

After this Introduction, this work is organized as follows: in Sec. II we discuss the model studied, its parametrization, and the methods of solution. Attention is paid to the questions of time scales, units, and the influence of initial conditions. In Sec. III results are presented for both the block-correlation functions and for the structure factor $C(q, t)$. The former are analyzed to show that there is scaling, and the growth laws are extracted from both the scaling analysis and by direct examination of the moments of $C(q, t)$, but the analysis of the latter is shown to be more difficult and less conclusive. The influence of the initial conditions and the zero-temperature limit are briefly discussed. The conclusions are recapitulated in Sec. IV. A preliminary analysis of the results reported here has been given in Ref. 13.

II. MODEL AND METHODS

A. Model

The model discussed here consists of a set of scalar fields, $\psi(\mathbf{R}, t)$, which for computational purposes are defined on the sites of a lattice. They can take values from $-\infty$ to $+\infty$. The equilibrium properties of the system are given by a Ginzburg-Landau free energy. We choose to parametrize this free energy as in Refs. 2 and 14, in which case it takes the form

$$F[\psi] = \frac{K}{2} \sum_{\mathbf{R}} \{ -\theta \psi^2(\mathbf{R}, t) + [\nabla \psi(\mathbf{R}, t)]^2 + \frac{1}{2}(1 + \theta) \psi^4(\mathbf{R}, t) \}, \quad (2.1)$$

where K represents the overall strength of the coupling, which we measure in units of temperature. The positive parameter θ measures the degree to which the static properties of the system are "Ising-like" or "displacive." In general, setting the gradient coefficient inside the sum in (2.1) equal to unity sets the unit of length.

The dynamics of this system, with a conserved order parameter, is given by a Langevin equation

$$\frac{\partial}{\partial t} \psi(\mathbf{R}, t) = \Gamma \nabla^2 \frac{\delta F[\psi]}{\delta \psi(\mathbf{R}, t)} + \eta(\mathbf{R}, t), \quad (2.2)$$

where Γ is a kinetic coefficient and our definition of the discrete Laplacian is given below by (2.5). We will usually set Γ equal to one, which establishes our unit of time. $\eta(\mathbf{R}, t)$ is a Gaussian noise field which satisfies the relation

$$\langle \eta(\mathbf{R}, t) \eta(\mathbf{R}', t') \rangle = -2\Gamma \nabla^2 \delta_{\mathbf{R}, \mathbf{R}'} \delta(t - t'), \quad (2.3)$$

which is consistent with the conservation law for the order parameter; i.e., the sum of $\psi(\mathbf{R}, t)$ over all space is a conserved quantity.

The physical quantities of interest in the context of the present work are various correlation functions. All of the correlation functions considered here are simply related to the basic two-point correlation function defined by

$$C(\mathbf{R}, \mathbf{R}', t) = \langle \psi(\mathbf{R}, t) \psi(\mathbf{R}', t) \rangle. \quad (2.4)$$

The angular brackets mean an average over the noise. In

practice, this average is carried out by solving the system of equations (2.2) as many times as necessary, with the noise terms being independently generated each time. One then averages over all the solutions found. Note that averaging over the initial probability distribution is also automatically carried out in the above procedure. We refer to each individual solution as a *run*.

B. Methods

The general procedure we have used here to solve the equations of the motion is the same as in Ref. 2. Here, we will only recapitulate briefly and emphasize the small differences imposed by the conservation law.

The numerical calculations were performed on a Cray 2 machine. In choosing algorithms and methods, a high priority was given to achieving a maximum degree of vectoring. It turns out that numerically simple routines which can be vectored are preferable to those more sophisticated but difficult to vector. The main integration procedure chosen was a simple Euler² method. Some of the advantages of this procedure over other methods were discussed in Ref. 2. For the Laplacians involved, the standard symmetric expression was used,

$$\nabla^2 \psi(\mathbf{R}, t) = \sum_a [\psi(\mathbf{R} + \delta_a, t) - \psi(\mathbf{R}, t)], \quad (2.5)$$

where δ_a is a set of vectors connecting a site to its nearest neighbors.

The generation of the noise field satisfying the correlation expression (2.3) was handled with the help of a method discussed in Ref. 7. The method, which makes use of the expression (2.5) for the Laplacian, involves the generation of two (in two dimensions) independent Gaussian fields, each with strength proportional to a δ function in space and time, which are combined to satisfy (2.5). This pair of fields was generated, as in Ref. 2, by using a numerical inversion of the probability function. The whole procedure was made into a single-vector loop. This greatly enhanced the overall numerical efficiency of the calculation.

The choice of initial conditions is not completely trivial in this case. For the most part, and following most previous work, we have made the simplest choice and set $\psi(\mathbf{R}, t=0) = 0$. Although this does not correspond to any specific equilibrium point in the (K, θ) phase diagram, it is very simple to use, and it does roughly represent some kind of disordered, high-temperature state. We have checked that the growth law is not unduly sensitive to the initial conditions by performing, in a few cases, a number of runs with random Ising initial conditions ($|\psi(\mathbf{R}, 0)|^2 = 1$) corresponding to initial equilibrium at the point $K=0, \theta=\infty$ in the phase diagram, and also with initial values of the fields uniformly distributed in the interval $(-v3, v3)$. This corresponds to displacive, high-temperature initial conditions with a cutoff. For quenches to $T=0$, the case $\psi(\mathbf{R}, t=0) = 0$ is trivial since one is led to the unstable solution $\psi(\mathbf{R}, t) = 0$, and one must use other initial conditions.

A question of interest is the connection between the time scale of the calculation discussed here (with $\Gamma=1$) and other perhaps more familiar units of time used in

computational physics, such as Monte Carlo steps (MCS's). Given the free-energy model (2.1) under consideration here, one can perform Monte Carlo simulations in the usual way: one considers a trial change in one of the fields $[\psi(\mathbf{R}, t)]$ and then accepts or rejects this change with a probability proportional to $\exp(-\delta F)$, where δF is the change induced in F by the trial change. It was shown in Ref. 15 that the results obtained for this model through the use of MC dynamics agree well with those obtained from solving Langevin equations provided that the magnitude of the trial change in the fields is taken to be sufficiently small. The question of the equivalence of the time scales was then explored in Ref. 15. The set of values for the free-energy parameters considered turns out to correspond to $K=7$, $\theta=2.5$ in the parametrization of Eq. (2.1). The computations out to 2200 MCS's were found to correspond to a "Langevin" time, $t=0.4$. Thus, a Langevin unit of time corresponds to 5500 MCS's at $K=7$, $\theta=2.5$. For other values of K and θ , one can form at least a fairly good idea of the correspondence in the following way: it turns out from our results that the time scale in which the system evolves is determined as one changes K mainly by the product $\tau=Kt$, with the θ dependence being less important. This could, in fact, be surmised from the form of the equations of the motion (2.2). Thus, one can roughly say that 2200 MCS's corresponds to $\tau=2.8$ and use this as an estimate of the corresponding MC scale.

A more difficult question would be the comparison of Langevin time scales for this model with MCS's for an Ising model with Kawasaki dynamics. The difficulty here is that although the static properties of the Ising model correspond to the model discussed as $\theta \rightarrow \infty$, the dynamics is quite different. One can only form a rough estimate by comparing the degree of order reached by the system at a certain time with corresponding Ising results. The results estimated in this way vary according to which quantity is chosen as the measure of order, but they are quite consistent with the numbers quoted in the preceding paragraph.

It should be emphasized that a large factor connects t and t_{MC} . An apparently small number in the Langevin scale corresponds to a large number of MCS's. It is important not to be misled by this when considering the time scales studied in this and similar work. A MCS is actually a very small unit, comparable to the integration step in a numerical method.

III. RESULTS

We consider here results obtained with the initial conditions discussed above after quenches to the ordered region of the phase diagram. This region is given in Refs. 2 and 14. The only parameters that one needs to choose are the values of K and θ corresponding to the final state, since the transport coefficient Γ merely establishes the units of time, as discussed in Sec. II. One must study a sufficient number of (K, θ) pairs to establish the ordered regime of the equilibrium phase diagram. The extent to which this can be done is limited by practical considerations.

The Langevin equations (2.2) are solved numerically on a square lattice (lattice structure is not expected to have any significant effect on the long time properties) typically containing 32×32 sites. We have verified, by checking larger and smaller sizes, that the results reported here are independent of the size of the system studied, as explained below. We have found that one must average over a substantial number of "runs" (~ 100) in order to obtain results of sufficiently good statistical quality for the correlation functions, so that one can reliably extract growth laws and static properties. It is therefore necessary to devise efficient ways to collect and analyze the information obtained about the correlations in the system as a function of time. For this reason we have performed most of our data collection and analysis in terms of block-correlation functions (the definition is given below). As shown in Refs. 16 and 17, the analysis of block-correlation functions offers a particularly efficient procedure to perform a scaling analysis of the results obtained by some numerical procedure in growth kinetics problems. An additional advantage in the present context is that the collection of block correlations is vectored easily. Therefore, we present in Sec. III A our numerical results for the block correlations and their analysis. However, we will subsequently give, in Sec. III B, a briefer account of a less complete but more standard type of analysis in terms of the structure factor $C(q, t)$. The tradition-minded reader may prefer to read these subsections in reverse order.

A. Block-correlation results

To define the block-correlation functions, we begin by considering blocks of size $M \times M$ embedded in the system of size $N \times N$ and $M < N$. We then define the block magnetization

$$m_M = \frac{1}{M^2} \sum_{\mathbf{R} \in M^2} \psi(\mathbf{R}, t), \quad (3.1)$$

and the block-correlation function

$$R_M(t) = \langle m_M^2 \rangle / S(t), \quad (3.2)$$

$$S(t) = \frac{1}{N^2} \sum_{\mathbf{R}} \langle \psi^2(\mathbf{R}, t) \rangle, \quad (3.3)$$

where the meaning of the brackets has been specified below (2.4). The factor of $S(t)$, which appears as a normalization factor, is the local-order parameter. Note that $S(t) \equiv 1$ for Ising variables. In the case of continuous variables, $S(t)$ is obviously not a constant for early times. In the present problem we find that $S(t)$ approaches its saturation value very rapidly when $\theta > K$ or $\theta \approx K$ and does not influence the longer time results for $R_M(t)$. However, when $\theta \ll K$, which means that the wall or gradient energy is dominant (thick-wall regime), the local-order parameter takes a relatively long time in reaching saturation. One then naturally wishes to separate the growth of the correlation functions due to the increase in domain size (which is the question of interest) from that merely due to the increase in the average value of ψ^2 . Normalizing by the factor given by (3.3) is a neat way of

achieving this separation.

From the definition (3.2) it follows that the $R_M(t)$ are essentially moments of the two-point correlation function (2.4), which is in turn the Fourier transform of $C(\mathbf{q}, t)$. It follows that the study of the block-correlation functions over an extended range of block sites is mathematically equivalent to a study of $C(\mathbf{R}-\mathbf{R}', t)$ or $C(\mathbf{q}, t)$.

We now turn to the question of how to extract scaling and growth law information from results for $R_M(t)$. First, in the scaling regime (if there is one) it is possible to write R in the form

$$R_M(t) = f(L(t)/M), \quad (3.4a)$$

where $L(t)$ is some characteristic length and f a scaling function. $L(t)$ may contain K and θ dependence. If one can establish (3.4a) by an analysis of $R_M(t)$, then one obtains $L(t)$ and $f(x)$. We note that the form (3.4a) cannot be expected to hold at very early times. It should also break down for sufficiently small values of M and also, because of the conservation law, when M becomes comparable with the overall size N .

We have obtained results for more than 12 pairs of values (K, θ) with K ranging from 0.8 to 14 and θ from 1.5 to 12. All of these points are well within the ordered region of the phase diagram.^{14,2} The results have been obtained for a system of size $N=32$ and for times $\tau=Kt$ ranging between 10 and 20. We emphasize once more that these are not short times: they are the equivalent of between about 10 000–20 000 MCS's per site. By performing additional runs at sizes $N=20, 25$ and (in some cases) $N=40$, we have verified that the results obtained are independent of N in the time ranges discussed here. Finite-size effects become apparent at the smaller values of N when one continues the integration to somewhat longer times. The first appearance of these effects in $R_M(t)$ has a characteristic signature discussed below. In all cases we have averaged our results over at least 100 runs. For any given M , run, and time bin, all possible blocks of size M in the system are collected, which produces a considerable additional averaging. Some of our raw data, chosen at random, are shown in Figs. 1 and 2. The scatter of the points with respect to a smooth curve is a measure of the quality of the data.

In all our data we find that starting at about $\tau \approx 1$, and up to the longest times considered, the quantity

$$F(M, t) = R_M(t)M^3 \quad (3.4b)$$

is independent of M for $7 < M < 18$ (this range is for $N=32$). An example of this can be seen in Figs. 3 and 4 where the same data as in Figs. 1 and 2 are replotted after multiplying the quantities plotted by M^3 . It can be seen that $F(M, t)$ is within statistical error independent of M for $M > 7$, while for the (K, θ) pairs exhibited in these figures, the $M=7$ values are still slightly different. Note that the results for even M , which were also obtained, are not plotted for clarity, so that by seeing the individual symbols, the reader can verify the lack of systematic M dependence. This property of $F(M, t)$ is also found for the kinetic Ising model with spin exchange¹⁷ and it can be seen (Appendix A) to follow from the conservation law.

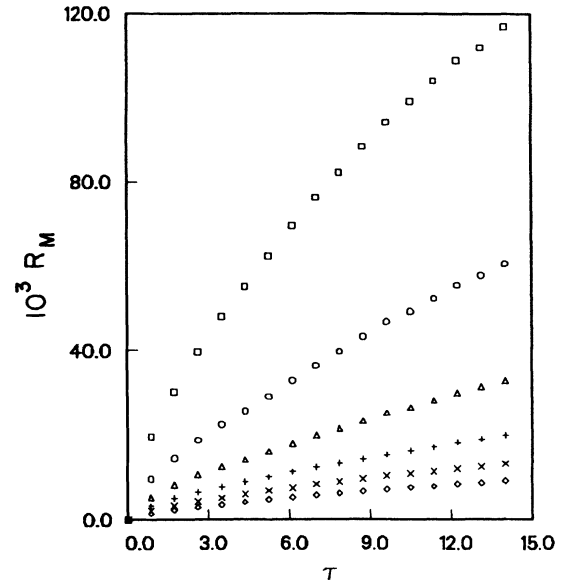


FIG. 1. An example of the raw data for the quantity $R_M(t)$ defined by (3.2). This quantity is plotted here for odd values of M ranging from $M=7$ (squares, top plot) to $M=17$ (diamonds, bottom plot) as a function of $\tau \equiv Kt$. The values of the quenching parameters are $K=1.75$, $\theta=2.5$. The smoothness of the plots (which correspond to 100 "run" averages) is an indication of the statistical quality of the data.

In Fig. 5 we exhibit this property for a wide range of K, θ and time values, covering a large portion of our results. The M independence of $F(M, t)$ can clearly be seen there.

The width of the M plateau increases with N . When working with smaller values of N at larger values of τ (which is then computationally easier), one observes that a signature or symptom of the first appearance of finite-size effects is the appearance of a sinusoidal waviness in

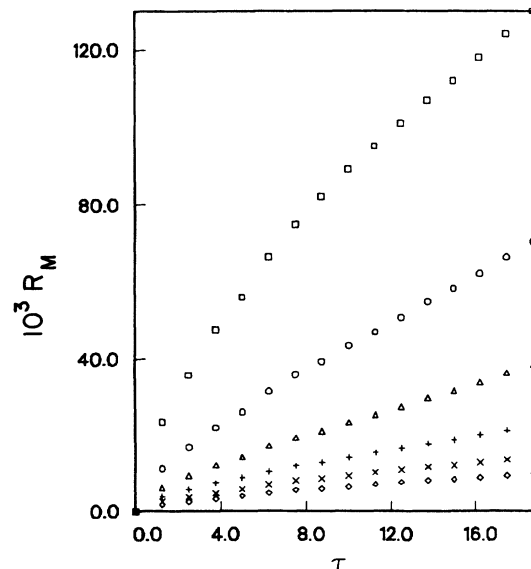


FIG. 2. Same as Fig. 1, but with $K=2.5$, $\theta=1.5$.

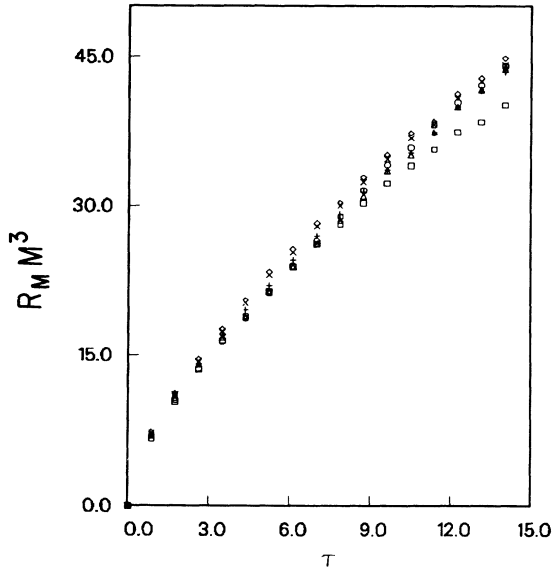


FIG. 3. The data shown in Fig. 1 replotted after multiplication by M^3 (see text). Note that all data with $M > 7$ fall on the same curve except for unsystematic statistical fluctuations. The symbols correspond to the same M values as in Fig. 1.

plots such as those in Fig. 5, which disappears (or, to be precise, shifts to longer times) when N is increased. This turns out to be quite useful as a warning signal.

Comparing Eqs. (3.4a) and (3.4b), we conclude that in the scaling regime one has

$$f(x) = x^3. \tag{3.5}$$

It is now convenient to introduce the quantity

$$D = - \frac{(\partial \ln R_M(t) / \partial \ln M)_t}{(\partial \ln R_M(t) / \partial \ln t)_M}, \tag{3.6}$$

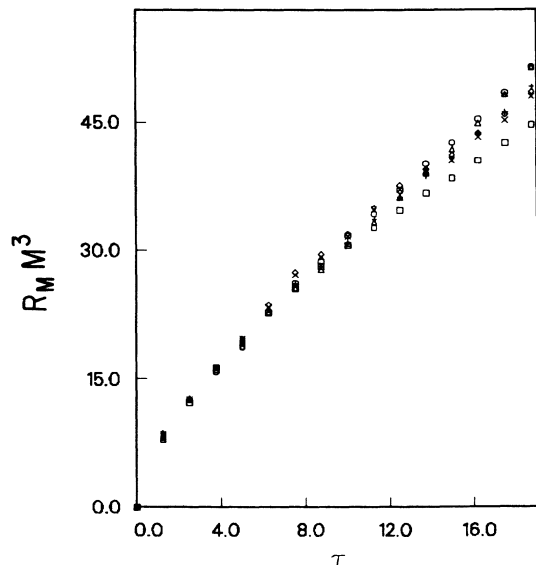


FIG. 4. Same as Fig. 3, for the data shown in Fig. 2.

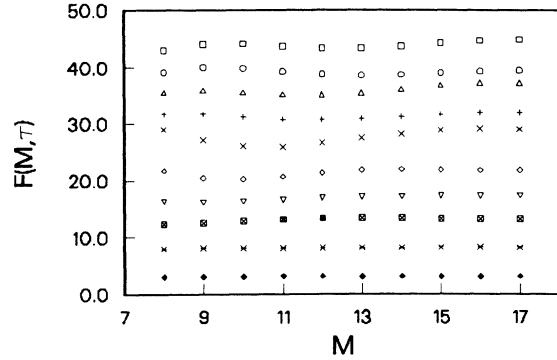


FIG. 5. The quantity $F(M, \tau)$ defined in (3.4) ($\tau \equiv Kt$) plotted as a function of M for the following values (from top to bottom) of (θ, K, τ) : (2.5, 1.75, 14), (1.5, 2.5, 13.75), (2.5, 1.75, 10.5), (1.5, 2.5, 10.0), (2.5, 2.5, 7.5), (5.0, 1.75, 5.25), (12, 0.8, 3.4), (12, 1.6, 3.2), (12, 0.8, 1.2), and (12.0, 3.2, 0.6). Note the monotonicity in τ which shows the weak (K, θ) dependence of $A(K, \theta)$ [see (3.8)].

and we see from (3.3)–(3.5) that if D is independent of time, then we are in the scaling regime and the characteristic length $L(t)$ varies with time according to a power-law result:

$$L(t) \approx t^n, \tag{3.7a}$$

$$n = 1/D. \tag{3.7b}$$

This analysis can be recast in a mathematically elegant way in terms of a Callan-Symanzik partial differential equation.^{16,17}

We find from our data that for all pairs of parameter values of (K, θ) we studied, D is a constant in time for $\tau \geq 3$ (in most cases, earlier). A representative sample of the data is plotted in Fig. 6. Two different vertical scales are used for clarity and emphasis. The average value of D over all the data shown in this figure is $D = 4.14 \pm 0.16$. This includes averaging over the different time bins in the time range where D is time independent. We conclude, therefore, that we have reached the scaling regime, that $L(t)$ varies with time according to a power law with exponent $n = \frac{1}{4}$. In fact, we find that we can write our results in the form

$$R_M(t) = [A(K, \theta) \tau^n / M]^3, \tag{3.8}$$

with $n = 1/D$, and where the amplitude A is a very slowly varying function of the parameters K, θ .¹⁸ This is why the plots in Fig. 5 are in order of increasing ξ , even though K and θ differ.

Although the main results obtained are independent of where we quench to in the phase diagram, some of the details are different. In particular, when $\theta \ll K$, the local-order parameter grows more slowly and the $S(t)$ normalization is important: without it the time region over which D is a constant is much reduced, and it would be difficult to reach definite conclusions. It can be seen from Eq. (3.3) that omitting the $S(t)$ normalization in the time region where $S(t)$ is still growing would obviously make no difference where $S(t)$ is constant but would decrease the value of D , which would then be somewhat

time dependent, that is, it would increase the value of the exponent n . The amount of this change depends on the logarithmic derivative

$$U(t) \equiv \frac{d \ln S(t)}{d \ln t}, \quad (3.9)$$

which we have plotted in Fig. 7 for the contrasting pairs of (K, θ) values. The difference would be even more striking if τ rather than t had been used for the horizontal scale.

If one erroneously omits the $S(t)$ normalization in the definition of $R_M(t)$ and the subsequent computations, the results for the regime $K \gg \theta$ (thick walls) change, but not in any other case. One then finds an appreciably long transient where $D < 4$ and, in fact, $n = 1/D$ seems compatible with $\frac{1}{3}$. This is exactly the opposite of the result found in a similar thick-wall regime in Ref. 11 for a different model, and therefore not the reason for the difference in the results.

All of the above results are obtained with zero initial conditions. In addition we have studied two pairs of (K, θ) values [(0.8, 12) and (1.75, 2.5)] with the other two types of boundary conditions discussed previously. The results in each case are in agreement with those obtained with standard initial conditions. However, the length of the initial time transients (before the scaling regime is

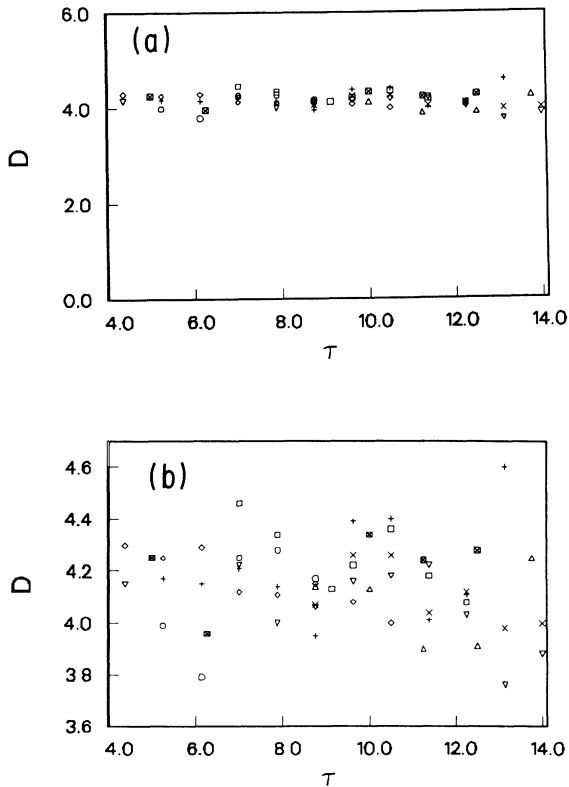


FIG. 6. The quantity D defined by (3.6) as a function of τ for the following values of (θ, K) : open squares (2.5, 14); circles (5, 1.75); triangles (2.5, 2.5); plus signs (2.5, 1.75); multiplication triangles (2.5, 3.5); and solid squares (1.5, 2.5). The two panels differ only on the vertical scale, which has been expanded in the second panel so that individual symbols can be distinguished.

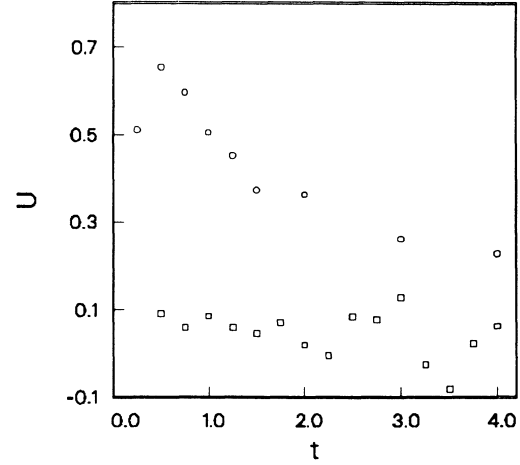


FIG. 7. The logarithmic derivative of the local order parameter as defined in (3.9) and (3.3), as a function of time. The circles correspond to $K \gg \theta$ ($K=10$, $\theta=1.5$) and the squares to the opposite limit ($K=0.8$, $\theta=12$).

reached) is increased. Furthermore, because one is now in effect averaging over different initial conditions, as well as noise, the statistical quality of the results suffers. We conclude that $\{\psi(\mathbf{R}, 0) = 0\}$ initial conditions are the most useful.

Finally, we also attempted to study the case of quenches to zero temperature, with both Ising and random initial conditions. To do this² one must set $K = J/T$ (where J is a coupling constant) and $\Gamma = \Gamma'T$, and measure the time in units of Γ' . As was the case for a non-conserved order parameter, the results are unsatisfactory. We found that it is difficult to obtain $R_M(t)$ results reasonably free of finite-size effects, and that there is no extended region where $L(t)$ varies according to a well-defined power law. Apparently, the presence of the noise term (which of course disappears at $T=0$) has a very profound effect on the properties of the model. Note that without the noise term one is simply averaging the solutions of a very nonlinear system of partial differential equations over a particular set of initial conditions, and this averaging becomes less efficient for longer times. It is possible that use of an extremely large number of runs would make the averaging over initial conditions equivalent to the noise averaging.

B. The structure factor

We now turn to a more traditional type of analysis in terms of the quasistatic structure factor, $C(q, t)$, defined as the Fourier transform of (2.4). We have obtained data for $C(q, t)$ for five pairs of (K, θ) values with K ranging from 0.8 to 6.4 and θ from 2.5 to 12. The data extend to time ranges comparable to those used for the block-correlation functions. In addition, results for $K=10$, $\theta=1.5$ were obtained up to a time $\tau=180$. This would correspond, according to the estimates presented earlier, to more than 140 000 MCS's. The results obtained are averages over 30 runs which, however, are at least as costly in terms of computer time as 100 runs for the block-correlation functions. The reason for this is that

the collection of the block information can be easily and very efficiently vectored in the Cray 2 computer. Two examples of the results obtained are given in Figs. 8 and 9 where the circular average of the quantity $C(q, t)$ is plotted at several times as a function of q_{eff}

$$q_{\text{eff}}^2 = [4 - 2(\cos q_x + \cos q_y)] , \quad (3.10)$$

which is the lattice equivalent of q^2 .

To obtain the growth law, one studies some characteristic wave vector as a function of time. One can, for example, consider $q_M(t)$, the position of the maximum in $C(q, t)$. The measurement of the position of the maximum is awkward since it must be extrapolated from the discrete set of $N \times N$ independent wave vectors that one has for a finite system. A better quantity to monitor is the first moment of $C(q, t)$

$$q_1(t) = \frac{\sum_q |q| C(q, t)}{\sum_q C(q, t)} , \quad (3.11)$$

which is preferable to any higher moments, since for the latter the influence of statistical noise in the high- q tail of the structure factor is larger. Computationally, we obtain $q_1(t)$ from the circularly averaged data. If we fit the results for either $q_M(t)$ or $q_1(t)$ to the form

$$q_c(t) = At^{-n} , \quad (3.12)$$

we obtain fairly good fits in all cases with an exponent n ranging from 0.21 to 0.28 and an overall average of $n = 0.26 \pm 0.02$. This is in agreement with the block-correlation results. In Fig. 10 we show the results for $q_1(t)$ obtained for the case $K = 10, \theta = 1.5$, where we obtained results for times up to $\tau = 180$.¹⁹ The best power-law fit, shown in the figure as the solid line, corresponds to $n = 0.27$.

However, it is important to point out that the results

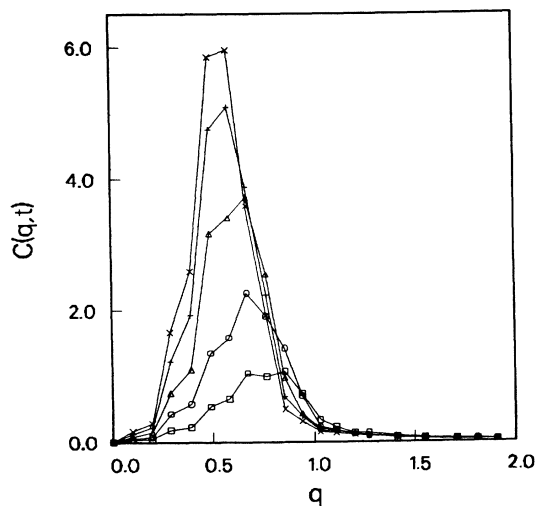


FIG. 8. An example of the results obtained for the structure factor $C(q, t)$. Here the circularly averaged $C(q, t)$ is plotted as a function of q_{eff} [see (3.10)]. The results correspond to 30 "run" averages at $K = 10, \theta = 1.5$, and the times shown are $\tau = 3.75, 6.25, 10, 13.75, \text{ and } 16.25$.

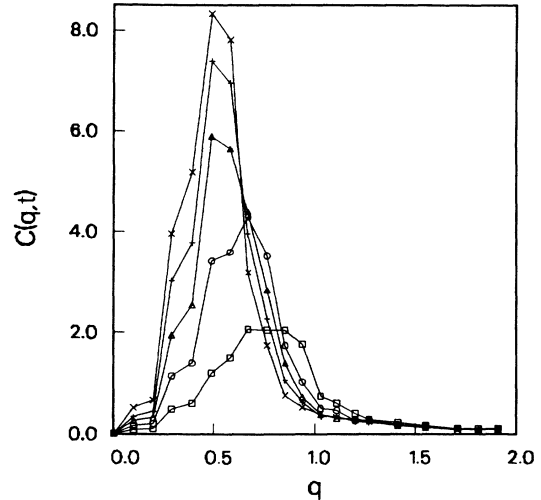


FIG. 9. Same as Fig. 8, but for $K = 3.5, \theta = 2.5$, and $\tau = 3.5, 7, 10.5, 14, \text{ and } 17.5$.

for $C(q, t)$ are not, by themselves, conclusive. This is partly due to statistical problems associated with the smaller number of runs and partly due to the absence of a mathematical method of systematic data analysis in space and time such as that developed for the block correlations. We find that fits nearly as good can also be obtained by fitting the chosen characteristic wave vector to alternative forms such as, for example, that used in Ref. 2:

$$q_c(t) = A(t - t_0)^{-n} \quad (3.13)$$

for many reasonable values of n (for example, $n = \frac{1}{3}$) provided one chooses the fairly small parameter t_0 appropriately. Similarly, fits to the form

$$q_c^{-1}(t) = A + Bt^n \quad (3.14)$$

are, for values of n in a range including $\frac{1}{3}$, not much worse than those of the form (3.12).²⁰ The values of A are, however, quite small [about 0.1 times the maximum value attained by $q_c^{-1}(t)$]. This is in contrast to early-time fits to data for the kinetic Ising model with spin exchange^{17,21} where the form (3.14) applies, but A is comparable to $q_c^{-1}(t)$. The fact that several fits are possible

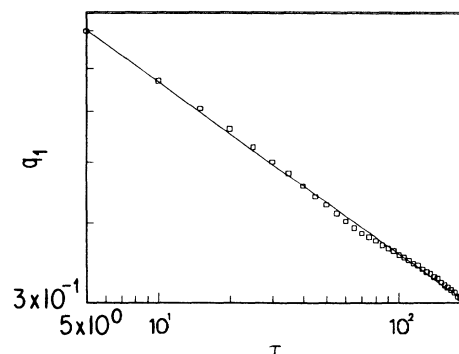


FIG. 10. The first moment of the structure factor [see (3.11)] as a function of τ for $K = 10, \theta = 1.5$.

reflects statistical problems; we find that data for a particular (K, θ) yielding a better quality fit to (3.12) (as measured by the coefficient of determination r^2) as compared to data for other choices of (K, θ) , also yield a better quality fit to the forms (3.13) and (3.14). This proves that the r^2 coefficient is measuring the quality of the data, rather than the quality of the fit.

We therefore regard these direct power-law fits as merely confirmatory, and agree with the authors of Ref. 8 in that it is not possible to obtain good exponent values from this type of analysis alone.

In the scaling regime, $C(q, t)$ can be written in the form

$$C(q, t) = C_M(t)F(q/q_M(t)). \quad (3.15)$$

As opposed to the situation with the block correlations, we have not been able to extract the scaling function $F(x)$ with sufficient accuracy to display it here. It appears that $F(x)$ has appreciable dependence on the parameters K and θ .

We have also obtained results (for $K = 1.75$, $\theta = 2.5$ only) with Ising and random boundary conditions. The comments made in this context in Sec. III A still apply. A similar situation holds concerning zero-temperature data.

We have seen in this subsection then, that a direct analysis of the structure factor is not practical or competitive in terms of computer resources used with the block-correlation analysis, although it is a useful check on the results.

IV. CONCLUSIONS

We have studied here the Langevin equation model for spinodal decomposition by direct numerical solution. We have found that, for a given expenditure of computer time, the block-correlation method is a much more efficient way of extracting scaling behavior and growth laws than the more standard analysis in terms of the structure factor.

We have seen that over the time scales considered here the system exhibits scaling behavior. The scaling function $f(x)$ for the block-correlation functions [see (3.4b)] is proportional to x^3 for small x , as motivated in the Appendix for a system with a conserved order parameter. Over this time scale, which must be considered at least as moderately long, the domains grow in time with an apparently time-independent exponent approximately equal to $\frac{1}{4}$. This behavior is in contrast with that of the kinetic Ising model with spin exchange where, over a comparable time range, the exponent n (or equivalently D) is strongly time dependent, increasing with time as $1/L(t)$ decreases. Such a dependence would appear as a decrease in D as a function of time [see (3.4a) and (3.6)], which we do not observe. It is obviously not possible to conclusively rule out a later change to a different value for the exponent, in which case the results reported here would correspond to a very long-lasting transient, the reason for which would have to be elucidated.

Since this work was submitted for publication there have been several brute-force simulations²² for the same

problem as studied here. In each case the authors strongly conclude that the growth law is $t^{1/3}$. While it might well turn out that the $t^{1/3}$ behavior is asymptotically correct, and the $t^{1/4}$ a transient, it is our opinion based on an analysis of their data and conversations with these authors, that the $t^{1/3}$ behavior has not yet been conclusively demonstrated. In any event, it appears that there is some regime where diffusion along an interface¹¹ and the associated $t^{1/4}$ behavior is present.

ACKNOWLEDGMENTS

A grant of computer time from the University of Minnesota Supercomputer Institute is gratefully acknowledged. This work was also supported by National Science Foundation Grant No. DMR 84-12901 at The University of Chicago.

APPENDIX: BEHAVIOR OF R_M FOR LARGE M FOR A CONSERVED ORDER PARAMETER

Assuming one can work in the continuum limit, (3.2) can be written as

$$R_M(t) = \frac{1}{S(t)M^4} \int_{-M/2}^{+M/2} d^2x \int_{-M/2}^{+M/2} d^2x' [C(\mathbf{x} - \mathbf{x}', t) - C(\mathbf{x} - \mathbf{x}', 0)],$$

where the integrals are over a square of side M . Eliminating $C(\mathbf{x} - \mathbf{x}', t)$ in terms of its Fourier transform and performing the \mathbf{x} and \mathbf{x}' integrations one obtains

$$R_M(t) = \int \frac{d^2q}{(2\pi)^2} \frac{C(\mathbf{q}, t)}{S(t)} \frac{4 \sin^2(q_x M/2) \sin^2(q_y M/2)}{M^4 q_x^2 q_y^2}.$$

Assuming that the dominant contribution to $C(\mathbf{q}, t)$ is isotropic, we obtain

$$R_M(t) = \int \frac{q dq}{(2\pi)^2} \frac{C(q, t)}{M^4 q^2 S(t)} I(qM/2),$$

where

$$I(x) = \int_0^{\pi/4} d\theta \frac{\sin^2(x \cos \theta) \sin^2(x \sin \theta)}{\cos^2 \theta \sin^2 \theta}.$$

We are interested here in the case of a conserved order parameter where $C(q, t)$ has a dominant peak at a nonzero value $q_M(t)$. We consider, then, the regime $q_M(t)M = M/L(t) \gg 1$, where we can take x large in the integral above. In this limit the main contribution comes from small θ and

$$\lim_{x \rightarrow \infty} \frac{I(x)}{x} = \frac{\pi}{2}.$$

Thus, to leading order in $L(t)/M (\ll 1)$,

$$R_M(t) = \frac{1}{M^3} \frac{\pi}{4} \int \frac{d^2q}{(2\pi)^2} \frac{C(q, t)}{q^3} / \int \frac{d^2q}{(2\pi)^2} C(q, t).$$

- ¹For comprehensive review, see, for example, J. D. Gunton, M. San Miguel, and P. S. Sahni, in *Phase Transitions and Critical Phenomena*, edited by C. Domb and J. L. Lebowitz (Academic, New York, 1983), Vol. 8; K. Binder, in *Statistical Physics*, edited by H. E. Stanley (North-Holland, Amsterdam, 1986).
- ²O. T. Valls and G. F. Mazenko, *Phys. Rev. B* **34**, 7941 (1986).
- ³P. C. Hohenberg and B. I. Halperin, *Rev. Mod. Phys.* **45**, 435 (1977).
- ⁴J. W. Cahn and S. M. Allen, *J. Phys. (Paris) Colloq. C* **7**, 5 (1977); S. M. Allen and J. W. Cahn, *Acta Metall.* **27**, 1085 (1979); I. M. Lifshitz, *Zh. Eksp. Teor. Fiz.* **42**, 1354 (1962) [*Sov. Phys.—JETP* **15**, 939 (1962)].
- ⁵A. Milchev, K. Binder, and D. W. Heermann, *Z. Phys. B* **63**, 521 (1986).
- ⁶The specific model considered here has been very extensively studied. See, among many examples, J. W. Cahn and J. E. Hilliard, *J. Chem. Phys.* **20**, 258 (1958); **31**, 668 (1959); J. S. Langer, M. Bar-on, and H. D. Miller, *Phys. Rev. A* **11**, 1417 (1975); K. Binder and D. Stauffer, *Phys. Rev. Lett.* **33**, 1006 (1974). The reviews in Ref. 1 have many additional pertinent references.
- ⁷R. Petschek and H. Metiu, *J. Chem. Phys.* **79**, 3443 (1983).
- ⁸A. Milchev, D. W. Heermann, and K. Binder (unpublished).
- ⁹G. F. Mazenko, O. T. Valls, and M. Zannetti, *Phys. Rev. B* **38**, 520 (1988).
- ¹⁰I. M. Lifshitz and V. V. Slyozov, *J. Chem. Sol.* **19**, 35 (1961).
- ¹¹Y. Oono and S. Puri, *Phys. Rev. Lett.* **58**, 836 (1987); *Phys. Rev. A* **38**, 434 (1988).
- ¹²M. Schobinger, S. W. Koch, and F. F. Abraham, *J. Stat. Phys.* **41**, 1071 (1986).
- ¹³G. F. Mazenko and O. T. Valls, *Phys. Rev. Lett.* **59**, 680 (1987).
- ¹⁴P. D. Beale, S. Sarker, and J. A. Krumhausl, *Phys. Rev. B* **24**, 266 (1981).
- ¹⁵P. Meakin, H. Metiu, R. G. Petschek, and D. J. Scalapino, *J. Chem. Phys.* **79**, 1943 (1983).
- ¹⁶G. F. Mazenko, O. T. Valls, and F. C. Zhang, *Phys. Rev. B* **32**, 5807 (1985).
- ¹⁷Z. W. Lai, G. F. Mazenko, and O. T. Valls, *Phys. Rev. B* **37**, 9481 (1988).
- ¹⁸This implies that any dependence of the scaling function f on the correlation length must be very weak. See Ref. 17 for a discussion of this question.
- ¹⁹The value of q_1 at the latest time shown in this figure is about the same as the minimum value of the same quantity attained in Ref. 11.
- ²⁰The values of the coefficient of determination r^2 decrease from typical values of about 0.998 to about 0.985.
- ²¹J. G. Amar, F. F. Sullivan, and R. D. Mountain, *Phys. Rev. B* **37**, 196 (1988).
- ²²T. M. Rogers, K. R. Elder, and R. C. Desai, *Phys. Rev. B* **37**, 9638 (1988); E. T. Gawlinski, J. Vinals, and J. D. Gunton (unpublished); R. Toral, A. Chakrabarti, and J. D. Gunton, *Phys. Rev. Lett.* **60**, 2311 (1988).